Tellus (1987), *39A*, 215–225

Reinterpretation of cloud-topped mixed-layer entrainment closure

By HOWARD P. HANSON, *Cooperative Institute for Research in Environmental Sciences, Campus Box 449, University of Colorado/NOAA, Boulder 80309-0449, USA*

(Manuscript received 3 June; in final form 5 November 1986)

ABSTRACT

Mixed-layer models of convective boundary layers in the atmosphere and oceans are powerful and useful tools for including important physical processes in general-circulation models of the two media as well as for diagnostic and prognostic studies of air-sea interaction and pollution dispersion. Recently, the appropriate physical and mathematical interpretation of the entrainment closure in such models has come under discussion. In mixed-layer ocean models and models of the dry convective atmospheric mixed layer, the discussion is essentially moot because, when the closure is implemented, its mathematics are independent of the physical interpretation. However, in mixed-layer models of the cloud-topped boundary layer, different physical interpretations lead to quite different mathematical formulations of the closure that yield widely differing results.

In this paper, a new interpretation of the turbulence energetics for the cloud-topped case is discussed. It retains the mathematical simplicity of an earlier approach while allowing consistency with recent numerical results concerning asymmetric diffusivities. Although the definitive study of the problem, by either theoretical, observational or numerical methods, remains for the future, the interpretation of turbulence energetics presented here is sufficiently flexible to be adaptable to new results.

1. Introduction

The convective boundary layers on both sides of the air-sea interface are the regions of atmosphere and ocean where the two media interact most strongly. The depth of these layers is determined by the turbulence energy available to entrain into the free atmosphere (ocean) above (below) the boundary layer across a stable inversion (thermocline). This entrainment process uses turbulence kinetic energy (TKE) to lift heavy fluid against gravity and, in the process, creates potential energy (PE). In an ideal, non-viscous fluid, the PE creation would occur conservatively, in the sense that PE at the entrainment interface would be created at the rate of TKE production elsewhere in the layer; the TKE production, in turn, occurs at the expense of PE released by an instability process. Ball (1960) first used this reasoning, coupled with arguments about turbulent eddy scales, to derive a simple mixed-layer model of the atmospheric boundary layer heated from below. He hypothesized that the turbulent eddies in the boundary layer are too large to be significantly affected by viscous dissipation and concluded that the downward heat flux at the layer top would be equal to the upward heat flux at the surface. Integrated over the depth of the layer, the net PE does not change in this case (Hanson, 1982). This, however, ignores the spectrum of turbulent eddies and the downscale transport of energy (that culminates in true viscous dissipation) in the turbulent boundary layer (e.g., Busch, 1973). Subsequent work in the early 1970's (Betts, 1973; Carson, 1973; Tennekes, 1973) modified Ball's approach to allow for dissipation, and it appears that most of the turbulence is dissipated and only a small amount is converted to PE by entrainment (Stull, 1976). While the original mixed layer ocean model of Kraus and Turner (1967) also adopted Ball's hypothesis, later formulations have allowed for dissipation in the ocean (e.g., Niiler and Kraus, 1977).

In the simplest case, the dry* atmospheric boundary layer heated from below, the effects of dissipation can be taken into account implicitly. This led to the straightforward parameterization

$$B_B = -\kappa B_S, \tag{1}$$

where B represents the buoyancy flux and subscripts B and S refer to the boundary-layer top and the surface, respectively. Ball's hypothesis sets $\kappa \equiv 1$; experimental and observational evidence suggests that $\kappa \sim 0.2$ is more realistic (e.g., Stull, 1976). The potential-energy analysis of Hanson (1982) showed how this implies that 80% of the TKE generated by surface heating is dissipated, and therefore only 20% is used for PE production at the top of the layer. From the perspective of energetics, the simple form of (1) is due to the layer's lack of internal sources and sinks of heat; i.e., there is no radiative flux convergence or condensation heating.

Both of these non-adiabatic processes are very important in cloud layers and this complicates the interpretation of the energetics. The purpose of this paper is to discuss the turbulent energetics for the case of the cloud-topped, well-mixed marine atmospheric boundary layer. In particular, this paper presents a new interpretation of the energetics, one that falls between two other interpretations that have arisen in the last decade or so. This new interpretation involves a reformulation of the turbulence closure that Randall (1984) has called "process partitioning". The reformulation, at the least, gives entrainment rates that are less inconsistent with those given by the other major candidate for closure, "Eulerian partitioning", than the earlier approach. In Section 2, a brief review of both closures and the reasoning behind the reformulation of process partitioning is presented. Section 3 discusses comparative results and the problem of cloud-top entrainment instability and Section 4 concludes the paper.

* "Dry" implies "undersaturated" here.

2. Entrainment in cloud-topped mixed-layer models

Entrainment parameterizations have been the subject of laboratory, field and theoretical research for many years. Much of this work has centered on formulating the entrainment as a function of an interfacial Richardson number. The choice of which Richardson number depends on the mechanism forcing the turbulence, and interpolation between extreme cases has been proposed to handle mixed-forcing situations (e.g., Deardorff, 1983). In the case of the cloud-topped mixed layer, the multiplicity of forcing mechanisms has thus far precluded any such approach to entrainment closure. Instead, integral methods based on the dry case forced by buoyancy fluxes (eq. 1) have been adapted for the cloud-topped case.

This discussion is confined to methods that involve partitioning the vertical integral of the buoyancy flux $B(z)$ in some fashion, as discussed by Randall (1984). Such a partitioning allows the sinks of TKE to be equated to some fraction of the TKE sources; the particular method of partitioning chosen defines these sources and sinks. In a dry mixed-layer model, the result (1) is obtained independently of the choice of partitioning methods discussed below.

The integral partitioning first discussed in the context of a dry model by Stull (1976) and then used in the cloud-topped case by Kraus and Schaller (1978), Randall (1980b), Fiedler (1984) and others, takes the source of TKE to be the integral of B over the part of the layer where $B > 0$ and the sinks to be the integral of B over that part of the layer where $B < 0$. Randall (1984) referred to this as "Eulerian" partitioning. In practice, this approach requires that the various levels where $B = 0$ be found; since these depend, in general, on w_e, the problem must be solved iteratively, except in special cases. This is a major drawback of the use of Eulerian partitioning in general-circulation models, where computational efficiency is a primary concern. Calculations using this method presented below are limited to simplified, linear radiative flux profiles.

Randall (1984) labeled the other main approach to integral closure "process" partitioning, because the effects of various physical processes on the entrainment rate are calculated separately. This approach was developed by Stage (1979) and by Hanson (1979) and is based on the physical argument that the creation of buoyant (light) and non-buoyant (heavy) parcels at various levels in the mixed layer is the result of various physical processes, the effects of which, for mathematical purposes, can be treated independently of each other. Thus, the effects of surface heating can be separated from the effects of radiative cooling when considering sources and sinks of TKE in the mixed layer. Although the mathematical formulation of process partitioning, as originally developed, is somewhat awkward, involving repeated use of rectifying functions (see Stage and Businger, 1981a, for a complete derivation), its numerical implementation turns out to be quite straightforward, as shown below, and requires no iteration. Unfortunately, as Randall (1984) pointed out, the original formulation is not unambiguous, and there is an element of arbitrariness in the exact method of partitioning. This problem is resolved below.

2.1. *Eulerian partitioning*

The integral closure introduced for the cloud-topped mixed layer model by Kraus and Schaller (1978) is formulated as

$$\langle B^- \rangle = \kappa^2 \langle B^+ \rangle, \tag{2}$$

where the angle brackets indicate a vertical integral over the mixed layer,

$$B^+ \equiv \Lambda(B); \tag{3a}$$

$$B^- \equiv \Lambda(-B), \tag{3b}$$

where Λ is the rectifier function:

$$\Lambda(x) = \begin{cases} x; & x > 0 \\ 0; & x \leqslant 0, \end{cases} \tag{4}$$

and where the dissipation constant κ [see eq. (1)] is squared to make the closure reduce to (1) for cases of dry or completely saturated (foggy) mixed layers. As Stage and Businger (1981a) and Hanson (1982) pointed out, this formulation implies that some 96% of the TKE in the layer is dissipated.

2.2. *Process partitioning*

The original process partitioning as formulated by Stage (1979) and by Hanson (1979) includes the contributions from the surface, cloud-top and infrared (IR) radiative fluxes separately. Further, the subcloud and cloud layer contributions from each of these were split. The vertical integral of the buoyancy flux B can be written, symbolically,

$$\langle B \rangle = \langle B \rangle^{S_1} + \langle B \rangle^{S_2} + \langle B \rangle^{B_1} + \langle B \rangle^{B_2} + \langle B \rangle^{F_1} + \langle B \rangle^{F_2} + \langle B \rangle^{G_1} + \langle B \rangle^{G_2} + \langle B \rangle^{P_1} + \langle B \rangle^{P_2} \equiv \Sigma \langle B \rangle^k \tag{5}$$

where

$$k = \{S_1, S_2, B_1, B_2, F_1, F_2, G_1, G_2, P_1, P_2\}.$$

The various superscripts represent terms from surface (S) and cloud-top (B) turbulent fluxes in the subcloud (1) and cloud (2) layers and non-adiabatic sources/sinks of buoyancy due to solar heating (F), IR cooling (G) and precipitation (P) in the two layers. Specific forms of the terms are given in Stage and Businger (1981a) and Hanson (1987); the specific forms of the terms associated with the non-adiabatic processes (F, G, P) depend on how the fluxes are formulated. The process closure takes

$$\langle B \rangle^+ = \sum_k \Lambda(\langle B \rangle^k), \tag{6a}$$

$$\langle B \rangle^- = -\sum_k \Lambda(-\langle B \rangle^k), \tag{6b}$$

$$\langle B \rangle^- = \kappa \langle B \rangle^+. \tag{7}$$

In this case, the interpretation of the fractional dissipation from the dry case (80%) is retained.

Randall's (1984) discussion of the closures pointed out a degree of arbitrariness in this form of process positioning. Some of this—involving the cloud-top IR cooling—has been addressed by the work of Nieuwstadt and Businger (1984), who showed how to formulate the cloud-top Reynolds' averaging to include all of the IR cooling within the mixed layer and by the observational study of Nicholls and Leighton (1986), who show that, in any case, the amount of IR cooling within the mean inversion is only a small fraction of the total. Other aspects of the arbitrary formulation are unresolved.

In particular, the splitting of the various terms into separate contributions in the two layers seems, at best, ad hoc. The fundamental assumption used in mixed-layer modeling is that the Reynold's-scale horizontally averaged quantities are invariant with height throughout the layer due to strong vertical mixing. This assumption leads directly to linearity of the vertical profiles of turbulent fluxes of conservative variables (with nonlinear terms contributed by non-adiabatic fluxes, Hanson, 1987). It then follows that the effects of the surface fluxes, for example, extend throughout the layer and there is no justification for singling out particular levels within the layer for special treatment. A similar argument applies to the cloud-top entrainment fluxes. Further, the effects of the internal non-adiabatic source and sink terms also extend throughout the layer with no preferred locations for their influence on the buoyancy partitioning (in an integrated sense).

From an observational perspective, there are two salient points to be considered. First, as Ball (1960) originally suggested, the dominant eddy scales are of the size of the layer depth, both for the dry and cloud-topped cases. This is well-documented in the dry case (e.g., Caughey, 1982); the data for cloud-topped mixed layers is less unequivocal, but the analysis by Brost et al. (1982) is suggestive in this regard. As a further example for the cloud-topped case, Fig. 1 shows smoothed power spectra of vertical velocity fluctuations at various levels within the mixed layer discussed in Hanson (1984a). (The measurements of velocity, by the NOAA/ERL gust probe system, Bean et al., 1976, are uncontaminated by cloud liquid water, unlike temperature or humidity.) In this case, the boundary-layer depth was 950 m, and cloud base was ~450 m. Note the dominance of scales in the 950–450 m bandwidth throughout the entire layer. The tendency toward smaller scales at the surface and layer top is expected due to the presence of a solid wall and a strong inversion, respectively. As discussed in Hanson (1984a), the cloud was absorbing ~125 W m^{-2} of solar energy and this was associated with a small entrainment rate. Hence, the velocity fluctuations near cloud top (at 920 m in Fig. 1) are much smaller than in mid-layer. Second, flight cameras and observer logs for flights into the cloud-topped mixed layer frequently show the lack of a clearly-defined cloud base. Rather, haze optical thickness gradually increases upward through the subcloud layer through the condensation level (which is "cloud base" in mixed-layer models) until the presence of cloud is unmistakable. It seems difficult to justify separating the turbulence in the cloud and

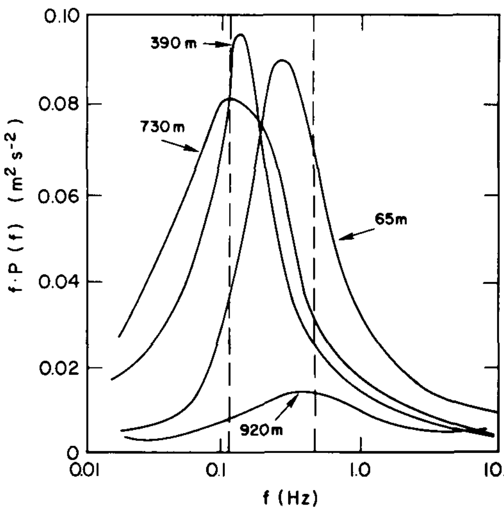

Fig. 1. Smoothed power spectra of vertical velocity fluctuations, obtained from ~40 km sampling runs, at various levels within the cloud-topped mixed layer discussed in Hanson (1984a). The dashed vertical lines enclose the 950–450 m spatial bandwidth.

subcloud layers for cases such as this. (The physical separation of the two layers that may occur due to solar heating—as discussed by Nicholls, 1984—is another matter altogether.)

While separation of sub-layers in the cloud-topped closure is thus questionable, there is reason to separate the effects of various *processes* that contribute to the net buoyancy flux. "Turbulence", after all, is simply the macro-scale view of individual events. Conditional sampling of the marine atmospheric boundary layer (Khalsa and Greenhut, 1985a) has shown these events to consist of plumes and/or thermals of varying intensity, buoyancy and origin. Upward plumes originating at the surface, due to positive buoyancy there, have different properties, particularly size and speed, from those originating higher up. It is to be expected that the transport efficiencies of the various categories of plumes differ. This expectation is borne out in numerical studies reported by Wyngaard and Brost (1984), who showed that "bottom-up" diffusion into a mixed layer operates distinctly differently from "top-down" diffusion. Also, Moeng (1985) has recently reported that the ratios of the PE-producing to TKE-producing eddies in a cloud-topped boundary layer modeled by the large-eddy technique differ for various forcing processes.

This ratio is related directly to the dissipation constant κ.

In the dry mixed-layer—where there are no internal sources or sinks of momentum or heat—it is useful to think of the turbulence in terms of a boundary-volume problem: the fluid responds to boundary forcing by developing motions over a spectrum of spatial scales. This boundary forcing can take the form of mechanical stresses or heat fluxes, and the fluid's response to the forcing depends on the forcing process. Although the properties of the fluid on the macroscale are affected by the net effect of all forcing processes (because of the mixing that is taking place), conditional sampling has shown that individual convective parcels retain an identity associated with a particular boundary forcing process through the entire depth of the layer (Khalsa and Greenhut, 1985b). Parcels exhibiting distinctly surface (inversion) characteristics are observed near the inversion (surface). While it is an obvious over-simplification to assert that these convective elements undergo no dilution, it is a useful—and reasonable—first-order approximation suitable for mixed-layer models.

Based on these arguments, it seems worthwhile to reformulate the original process partitioning closure using the following reasoning: the buoyancy flux in a well-mixed layer is influenced by two types of processes, viz., boundary processes and internal processes. Since there are two boundaries, there are three relevant terms in a closure formulation, involving surface buoyancy fluxes, cloud-top entrainment fluxes and internal sources and sinks. Thus, defining

$$\langle B\rangle^{S} \equiv \langle B\rangle^{S_1} + \langle B\rangle^{S_2} \tag{8a}$$

$$\langle B\rangle^{B} \equiv \langle B\rangle^{B_1} + \langle B\rangle^{B_2} \tag{8b}$$

$$\langle B\rangle^{Q} \equiv \langle B\rangle^{F_1} + \langle B\rangle^{F_2} + \langle B\rangle^{G_1} + \langle B\rangle^{G_2} + \langle B\rangle^{P_1} + \langle B\rangle^{P_2} \tag{8c}$$

and

$$l \equiv \{S, B, Q\},$$

leads to

$$\langle B\rangle^{+} = \sum_{l} \Lambda(\langle B\rangle^{l}), \tag{9a}$$

$$\langle B\rangle^{-} = \sum_{l} \Lambda(-\langle B\rangle^{l}). \tag{9b}$$

The closure then uses eq. (7). Comparison of (6) and (8) will show how this new formulation will lead to larger entrainment rates in the presence of, for example, solar heating. In this case $\langle B\rangle^{F_1}$, $\langle B\rangle^{F_2} < 0$ and the sum of the radiative-flux forcing in (7) (assuming a positive IR contribution) is $\kappa\{\langle B\rangle^{G_1} + \langle B\rangle^{G_2}\} - \langle B\rangle^{F_1} - \langle B\rangle^{F_2}$. With the new partitioning, the last two (solar) terms are included in the braces and their negative contribution is decreased by a factor of $1/\kappa$. It is useful to note that IR cooling that may occur within the mean inversion can be included as boundary forcing in the $\langle B\rangle^{B}$ term. In the computations below, it is assumed that all of the IR cooling occurs within the mixed layer.

3. Discussion

The results of calculations comparing the behavior of the entrainment closures are presented in this section. In order to facilitate labeling, the following abbreviations are introduced for the closures discussed above:

- EP for the Eulerian partitioning (Kraus and Schaller, 1978) (solid curves in the figures);
- PP1 for the original formulation of the process partitioning (Stage and Businger, 1981a, b) (short-dashed curves); and
- PP2 for the new process partitioning in eqs. (8) and (9) (long-dashed curves).

It is useful to note that, without cloud-base IR warming or solar heating, with a positive surface buoyancy flux, and in the absence of cloud-top entrainment instability (CEI; Deardorff, 1980), PP1 and PP2 are identical.

Because the iteration needed to solve the EP closure is very complicated with realistic radiative flux profiles, the closures are compared here using linear radiative flux profiles derived from the exponential profiles of Hanson (1987). The cloud-base warming is neglected, and the cloud-top cooling is assumed to occur over several tens of meters near cloud top; the exact height interval is derived form the more precise, exponential profiles by requiring the net buoyancy forcing of the two (linear and exponential) profiles to match. The solar heating is assumed to be constant throughout the cloud (i.e., the solar flux profile is linear) with the same net amount of heating as predicted by the parameterization. By spreading the solar heating over the entire depth of the cloud, rather than over its upper half or so as predicted by radiative transfer theory, the solar heating becomes less efficient at impeding turbulence generation (Hanson, 1987). This is exacerbated by the neglect of cloud-base IR warming, which, for mixed layers with cloud base above the layer's center of mass, also impedes turbulence generation.

The basic geometry of the layer and the boundary conditions, typical of the cloud-topped marine atmospheric boundary layer off the west coast of North America, are listed in Table 1. Calculations below compare the sensitivity of the closures to variations in several parameters about the values in Table 1. These include the sea-surface temperature (SST), which controls the surface fluxes, the downward cloud-top IR flux, solar heating (as controlled by the solar zenith angle), cloud thickness (which implicitly controls the net effect of latent heat release on the layer's turbulence budget as well as the solar absorption and IR emission), the cloud-base height as controlled by the layer's moisture content and the relative humidity of the air above the inversion (which partly controls the onset of CEI). These quantities are all specified in the calculations, and there are no assumptions (such as horizontally homogeneous or steady-state conditions) made about the layer budgets. Details of the thermodynamic model used here can be found in Hanson (1987).

3.1. Sensitivity to layer geometry and forcing

It will be seen that the EP closure yields entrainment rates that are consistently about twice as large as the PP2 closure. This has also been noted by Nicholls and Turton (1986) in a comparison of various closures (including those of Schubert, 1976 and Deardorff, 1976 as well as EP and PP1) with observations; with the exception of one case, the EP closure agreed fairly well with the observations. The emphasis in this paper is on the sensitivity of the closures. Because the value of the dissipation constant κ is not well-known (and, based on the previous discussion, it may not even be a constant) for cloud-topped mixed layers, it must be considered adjustable. Hence, the consistently-higher entrainment rates from the EP closure may simply be related to this obscurity of κ. This possibility is strengthened when the Nicholls and Turton (1986) results are examined in detail: if the PP1 and EP entrainment rates are regressed against the observed entrainment rates (eliminating the single bad case), the slopes of the regression lines are 0.72 and 0.68, respectively, and the intercepts are -0.08 and 0.10. (A perfect fit would, of course, have a slope of 1.0 and an intercept of 0.) The slopes of these regression lines, which represent the sensitivity of the closures, are in good agreement. The small number of cases (4) makes further statistical analysis unreliable: more observations are clearly needed.

Figs. 2 compare the behavior of the closures

Table 1. *Basic forcing and boundary conditions*

Quantity	Symbol	Value
Surface conditions		
Sea surface temperature	T_S	289 K
Surface air temperature	T_A	288 K
Surface air relative humidity	RH_A	85%
[This implies cloud base	z_C	$\sim$350 m]
10-m wind speed	U_A	5 m s^{-1}
Cloud top height	z_B	$z_C + 300$ m
Upper air conditions		
Temperature	T_U	$294.5 - 0.0048 z_C$
Relative humidity	RH_U	30%
Downward IR flux	$G\downarrow_B$	275 W m^{-2}
Downward (direct beam) solar flux	$F\downarrow_B$	500 W m^{-2}
Solar zenith angle cosine	μ_0	0.5

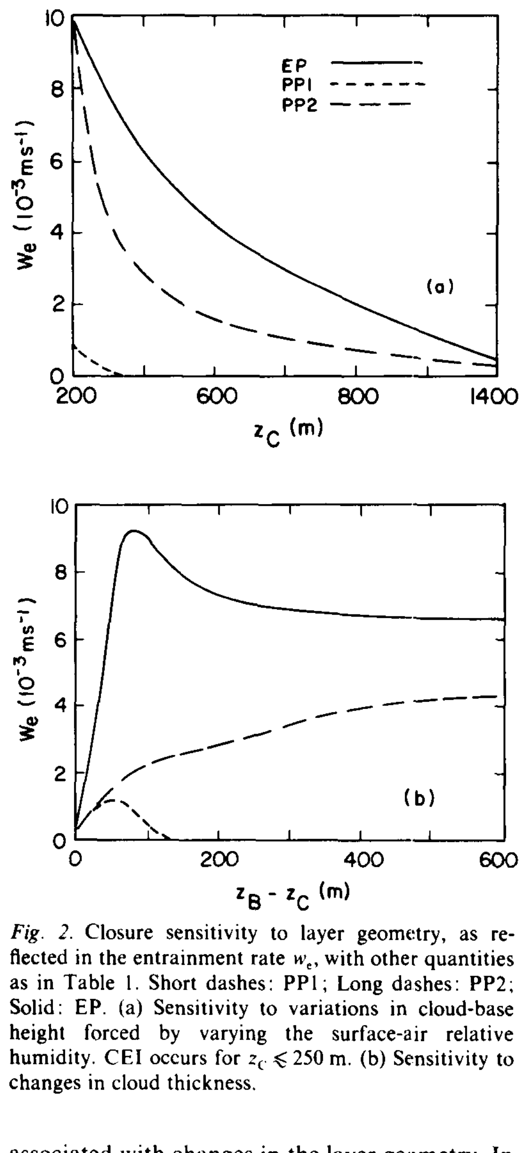

Fig. 2. Closure sensitivity to layer geometry, as reflected in the entrainment rate w_e, with other quantities as in Table 1. Short dashes: PP1; Long dashes: PP2; Solid: EP. (a) Sensitivity to variations in cloud-base height forced by varying the surface-air relative humidity. CEI occurs for $z_C \leqslant 250$ m. (b) Sensitivity to changes in cloud thickness.

associated with changes in the layer geometry. In Fig. 2a, the results of varying the cloud-base height show consistent behavior among the three closures, with the PP1 method predicting non-zero entrainment only for very low bases. In order to keep the layer thermodynamics consistent, the variations of cloud base were forced by changing the layer's moisture content; therefore the surface fluxes and the inversion strength also changed. The large increase in entrainment for the smaller values of cloud-base height is due to the onset of CEI below about $z_C = 300$ m. This will be discussed further below. Fig. 2b presents results for variable cloud thickness. In this case, the absorbed solar radiation, the emitted IR radiation and the (implicit) latent heat release vary. IR cooling increases quite rapidly for small cloud thicknesses; at some point solar heating begins to become significant. This explains the maxima in the EP and PP1 entrainment rates. The PP2 closure is considerably more robust with respect to solar heating, as discussed above, and the gradual increase of w_e with increasing cloud thickness is only slowed by the increasing solar heating. Both the EP and PP2 entrainment rates level off for very thick clouds, because the effects of the radiative fluxes effectively saturate. This is also discussed in Hanson (1987).

The closures' sensitivities to changes in forcing are illustrated in Figs. 3. In Fig. 3a, the effects of varying the SST are shown; over the range of SST's shown, the total heat flux (i.e., the moist static energy flux) increased from about 15 to 145 W m^{-2}. The solar heating, in the basic state forcing (Table 1), is sufficiently strong to prevent entrainment in the PP1 closure. As the surface fluxes increase, eventually enough energy is available to overcome the stabilization of the solar heating, and PP1 predicts entrainment for SST's above about 20°C. The other two closures predict entrainment throughout the range of SST's shown; the faster increase below 17.5°C is due to a change in the sign of the surface buoyancy flux. Analogous to surface heating, cloud-top cooling also generates turbulence. The closures' sensitivities to changing the downward IR flux at cloud top are shown in Fig. 3b (the upward component is calculated from the cloud thickness and the cloud-top temperature). The sensitivity patterns for the three closures are similar for these two turbulence forcing mechanisms: PP1 requires substantial energy to overcome its treatment of the solar heating, and PP2 is somewhat less sensitive than EP. This is repeated in an inverse sense for varying solar heating (which was accomplished by varying the solar zenith angle in the calculation), as shown in Fig. 3c. The greater sensitivity of the EP closure than PP1 to changes in surface-flux forcing was also noted by Nicholls and Turton (1986).

3.2. *Cloud-top entrainment instability*

As originally formulated by Deardorff (1980)

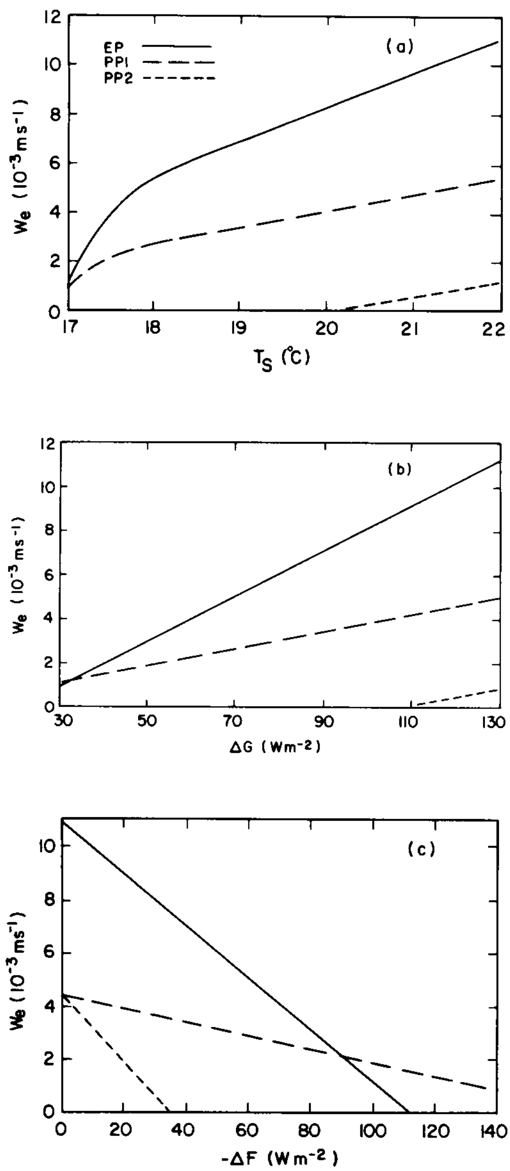

Fig. 3. Closure sensitivity to changes in layer forcing, conventions as in Fig. 1. (a) Changing SST. (b) Changing cloud-top IR flux. (c) Changing solar heating (forced by varying the solar zenith angle).

and Randall (1980a), the onset of CEI was hypothesized to lead to the break-up of a solid cloud deck. The mechanism of CEI is the entrainment of air parcels into the cloud that are sufficiently dry that they become non-buoyant with respect to cloud-top air before they become saturated. When this happens, the entrainment process becomes a generating mechanism for TKE, rather than a sink of TKE. Hanson (1982) suggested that a criterion based on the onset of CEI may be an insufficient indicator of the imminent break-up of a solid cloud and Hanson (1984b) showed that the CEI mechanism alone does not conform to observations. Other work by Albrecht et al. (1985) and Nicholls and Turton (1986) has supported this conclusion. Hanson (1984b) introduced the concept of the zero-buoyancy level within a cloud of the parcels entrained; it turns out that just-saturated parcels are the heaviest, so the most conservative measure of the potential penetration into a cloud of a parcel undergoing CEI pertains to just-saturated mixtures of cloud and upper air. Nicholls and Turton (1986) recently introduced a similar measure based on the average of all possible mixtures that is somewhat less conservative than the zero-buoyancy level for just-saturated mixtures.

This zero-buoyancy level, normalized by the cloud thickness, is denoted by ψ; $\psi = 0$ corresponds to cloud base and $\psi = 1$ to cloud top. CEI occurs for $\psi < 1$. Fig. 4 show the sensitivity of the entrainment rates predicted by the three closures to changes in ψ, which were forced by varying the relative humidity of the above-inversion air. Fig. 4a pertains to the conditions in Table 1 (with variable upper-air humidity), for which closure PP1 never predicts entrainment, and Fig. 4b pertains to identical conditions with no solar radiation. In the latter case, PP1 is identical to PP2 for $\psi > 1$, as mentioned previously. In contrast to the previous results, the sensitivity of the PP2 closure is markedly greater during CEI than that of the other two. This can be traced to the difference between eqs. (6) and (9).

Another candidate for the mechanism of stratocumulus instability (i.e., the break-up of a solid cloud deck) was suggested by Deardorff (1980) to be the increased drying of the cloud that would accompany increased entrainment. Since the entrainment increases with the onset of CEI, the two mechanisms could be coincident. However, they are physically distinct. CEI is a buoyant instability; Deardorff's increased drying is associated simply with the cloud's evaporating. Hanson (1984b) formulated the ratio T of the time scales of cloud moistening by mixing from

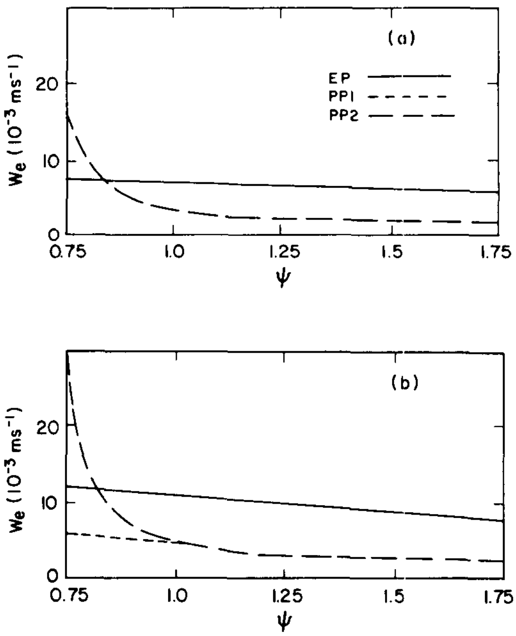

Fig. 4. Closure sensitivity to CEI, forced by varying the upper-air humidity, as a function of the normalized zero-buoyancy level for just-saturated entrained mixtures, with (a) and without (b) solar heating. Conventions as in Fig. 1.

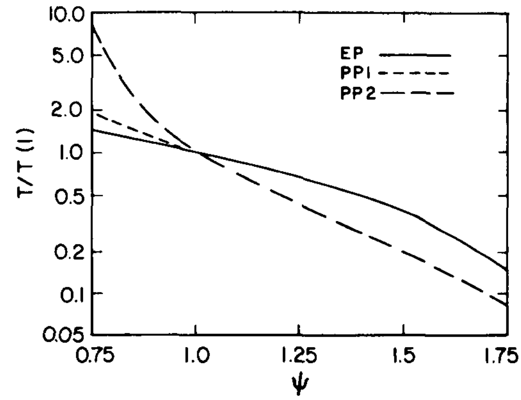

Fig. 5. Sensitivity of time-scale ratio to CEI, as in Fig. 4b.

below and cloud drying by entrainment for a mixed layer model and showed that the ratio increases after the onset of CEI, implying that the drying time scale decreases and drying should dominate. Fig. 5 shows the behavior of this ratio, normalized by the ratio for neutral conditions ($\psi = 1$) for the three closures. The EP closure is the least sensitive of the three closures, and, due to the differences between eqs. (6) and (9), the PP2 closure is very sensitive. There are insufficient observations to validate this calculation, although Nicholls and Turton's (1986) results indicate a relatively large value of T for their single CEI case.

4. Conclusion

Pending a unified theory of turbulent entrainment that includes the various non-adiabatic processes important to cloud dynamics, it is likely that integral parametrizations, such as those developed by Kraus and Schaller (1978) or Stage (1979) and Hanson (1979) will play a crucial rôle in boundary-layer modeling. This paper has presented a reinterpretation of the closure called by Randall (1984) *process partitioning*. In the original formulation, the effects of various processes that affect the turbulent buoyancy flux were separated by the sub-layer in which they act as well as by process. In the new interpretation, the cloud and subcloud layers are not considered separately, and all processes are classed according to their contributions as *boundary* forcing or as *internal* forcing.

Arguments for partitioning the buoyancy flux by processes include evidence from numerical experiments that indicate the efficiencies of different processes may differ (e.g., Wyngaard and Brost, 1984) and observations that turbulent events of various buoyant and non-buoyant categories occur at all levels within the boundary layer (Khalsa and Greenhut, 1985b). Lumping the effects of all processes together, as in the Eulerian partitioning (Randall, 1984) oversimplifies the mechanics of the boundary layer. Arguments against separating the turbulence energetics in the subcloud and cloud layers include observations of the size of eddies in the cloud-topped mixed layer and, more basically, the concept of a "mixed layer".

The sensitivity of the new interpretation of process partitioning to layer geometry and forcing is consistent with that of the earlier interpretation (Stage and Businger, 1981a, b) and somewhat less than that of the Eulerian closure. On the other hand, process partitioning is more sensitive to the onset of cloud-top entrainment instability than Eulerian partitioning, and the new method is very sensitive. More observations of cloud-topped marine boundary layers are needed to determine the sensitivity of the real atmosphere to the onset of this process.

5. Acknowledgements

This paper resulted from research supported by the U.S. National Science Foundation under grant ATM 82-09115 and by the U.S. Office of Naval Research under Contract N00014-84-K-0405. The data in Fig. 1 were obtained under sponsorship of the U.S. National Oceanographic and Atmospheric Administration's Equatorial Pacific Ocean Climate Studies program. Discussions with Professor Steven A. Stage, of the Florida State University, provided valuable insight into the ideas presented here.

REFERENCES

Albrecht, B. A., Penc, R. S. and Schubert, W. H. 1985. An observational study of cloud-topped mixed layers. *J. Atmos. Sci. 42*, 800–822.

Ball, F. K. 1960. Control of inversion height by surface heating. *Q. J. R. Meteorol. Soc. 86*, 483–494.

Bean, B. R., Gilmer, R. O., Hartman, R. F., McGavin, R. E. and Reinking, R. F. 1976. Airborne measurement of vertical boundary layer fluxes of water vapor, sensible heat and momentum during GATE. NOAA Technical Memorandum ERL WMPO-36. NOAA/ERL, Boulder, CO, 83 pp.

Betts, A. K. 1973. Non-precipitating cumulus convection and its parameterization. *Q. J. R. Meteorol. Soc. 99*, 178–196.

Brost, R. A., Wyngaard, J. C. and Lenschow, D. H. 1982. Marine stratocumulus layers. Part II: Turbulence budgets. *J. Atmos. Sci. 39*, 818–836.

Busch, N. E. 1973. On the mechanics of atmospheric turbulence. In: *Workshop on Micrometeorology*, Ed. D. A. Haugen, Am. Meteor. Soc., Boston, 1–68.

Carson, D. J. 1973. The development of a dry inversion-capped convectively unstable boundary layer. *Q. J. R. Meteorol. Soc. 99*, 450–467.

Caughey, S. J. G. 1982. Observed characteristics of the atmospheric boundary layer. In: *Atmospheric turbulence and air pollution modelling*, F. T. M. Nieuwstadt and H. van Dop, eds., D. Reidel Publishing, Dodrecht, pp. 107–158.

Deardorff, J. W. 1976. On the entrainment rate of a stratocumulus-topped mixed layer. *Q. J. R. Meteorol. Soc. 102*, 563–582.

Deardorff, J. W. 1980. Cloud top entrainment instability. *J. Atmos. Sci. 37*, 131–147.

Deardorff, J. W. 1983. A multi-limit mixed-layer entrainment formulation. *J. Phys. Oceanogr. 13*, 988–1002.

Fiedler, B. H. 1984. The mesoscale stability of entrainment into cloud-topped mixed layers. *J. Atmos. Sci. 41*, 92–101.

Hanson, H. P. 1979. Response of subtropical marine boundary-layer cloudiness to large-scale forcing. Ph.D. Dissertation, University of Miami, Coral Gables, FL, 148 pp.

Hanson, H. P. 1982. Note on mixed-layer entrainment closure. *J. Atmos. Sci. 39*, 470–473.

Hanson, H. P. 1984a. On mixed-layer modeling of the stratocumulus-topped marine boundary layer. *J. Atmos. Sci. 41*, 1226–1234.

Hanson, H. P. 1984b. Stratocumulus instability reconsidered: a search for physical mechanisms. *Tellus 36*, 355–368.

Hanson, H. P. 1987. Radiative/turbulent transfer interactions in layer clouds. *J. Atmos. Sci. 44*, in press.

Khalsa, S. J. S. and Greenhut, G. K. 1985a. Conditional sampling of updrafts and downdrafts in the marine atmospheric boundary layer. *J. Atmos. Sci. 42*, 2550–2562.

Khalsa, S. J. S. and Greenhut, G. K. 1985b. Conditional sampling of penetrative updrafts and entraining downdrafts near the top of the marine atmospheric boundary layer. *Seventh Symposium on Turbulence and Diffusion of the American Meteorological Society, Extended Abstracts*, 55–58.

Kraus, E. B. and Turner, J. S. 1967. A one-dimensional model of the seasonal thermocline: II. The general theory and its consequences. *Tellus 19*, 98–106.

Kraus, H. and Schaller, E. 1978. A note on the closure in Lilly-type inversion models. *Tellus 30*, 284–288.

Moeng, C.-H. 1985. An application of large-eddy simulation to mixed-layer modeling. *Seventh Symposium on Turbulence and Diffusion of the American Meteorological Society, Extended Abstracts*, 353–356.

Nicholls, S. 1984. The dynamics of stratocumulus: aircraft observations and comparisons with a mixed-layer model. *Q. J. R. Meteorol. Soc. 110*, 783–820.

Nicholls, S. and Leighton, J. 1986. An observational study of the structure of stratiform cloud sheets. Part I. *Q. J. R. Meteorol. Soc. 112*, 431–460.

Nicholls, S. and Turton, J. D. 1986. An observational study of the structure of stratiform cloud sheets. Part II. Entrainment. *Q. J. R. Meteorol. Soc. 112*, 461–480.

Nieuwstadt, F. T. M. and Businger, J. A. 1984. Radiative cooling near the top of a cloudy mixed layer. *Q. J. R. Meteorol. Soc. 110*, 1073–1078.

Niiler, P. P. and Kraus, E. B. 1977. One-dimensional models of the upper ocean. In: *Modelling and Prediction of the Upper Layers of the Ocean*, Ed. E. B. Kraus, Pergamon, Oxford, 143–172.

Randall, D. A. 1980a. Conditional stability of the first kind upside-down. *J. Atmos. Sci. 37*, 125–130.

Randall, D. A. 1980b. Entrainment into a strato-cumulus layer with distributed radiative cooling. *J. Atmos. Sci. 37*, 148–159.

Randall, D. A. 1984. Buoyant production and consumption of turbulence kinetic energy in cloud-topped mixed layers. *J. Atmos. Sci. 41*, 402–413.

Schubert, W. H. 1976. Experiments with Lilly's cloud-topped mixed layer model. *J. Atmos. Sci. 33*, 436–446.

Stage, S. A. 1979. A Model for Modification of the Cloud-Topped Marine Boundary Layer during Cold Air Outbreak. Ph.D. Dissertation, University of Washington, Seattle, 280 pp.

Stage, S. A. and Businger, J. A. 1981a. A model for entrainment into a cloud-topped marine boundary layer. Part I: Model description and application to a cold-air outbreak episode. *J. Atmos. Sci. 38*, 2213–2229.

Stage, S. A. and Businger, J. A. 1981b. A model for entrainment into a cloud-topped marine boundary layer. Part II: Discussion of model behavior and comparison with other models. *J. Atmos. Sci. 38*, 2230–2242.

Stull, R. B. 1976. The energetics of entrainment across a density interface. *J. Atmos. Sci. 33*, 1260–1267.

Tennekes, H. 1973. A model for the dynamics of the inversion above a convective boundary layer. *J. Atmos. Sci. 30*, 558–567.

Wyngaard, J. C. and Brost, R. A. 1984. Top-down and bottom-up diffusion of a scalar in the convective boundary layer. *J. Atmos. Sci. 41*, 102–112.